Spectroscopic characterization of the excitation energy transfer in the fucoxanthin–chlorophyll protein of diatoms

Emmanouil Papagiannakis[1],*, Ivo H.M. van Stokkum[1], Holger Fey[2], Claudia Büchel[2] & Rienk van Grondelle[1]

[1]*Department of Physics and Astronomy, Faculty of Sciences, Vrije Universiteit, De Boelelaan 1081, 1081 HV Amsterdam, The Netherlands;* [2]*Institute of Botany, University of Frankfurt, Siesmayerstrasse 70, 60323 Frankfurt, Germany;* *Author for correspondence (e-mail: papagian@nat.vu.nl; fax: +31-20-5987999)*

Abstract

We characterized the energy transfer pathways in the fucoxanthin–chlorophyll protein (FCP) complex of the diatom *Cyclotella meneghiniana* by conducting ultrafast transient absorption measurements. This light harvesting antenna has a distinct pigment composition and binds chlorophyll *a* (Chl-*a*), fucoxanthin and chlorophyll *c* (Chl-*c*) molecules in a 4:4:1 ratio. We find that upon excitation of fucoxanthin to its S_2 state, a significant amount of excitation energy is transferred rapidly to Chl-*a*. The ensuing dynamics illustrate the presence of a complex energy transfer network that also involves energy transfer from the unrelaxed or 'hot' intermediates. Chl-*c* to Chl-*a* energy transfer occurs on a timescale of a 100 fs. We observe no significant spectral evolution in the Chl-*a* region of the spectrum. We have applied global and target analysis to model the measured excited state dynamics and estimate the spectra of the states involved; the energy transfer network is discussed in relation to the pigment organization of the FCP complex.

Abbreviations: Chl – chlorophyll; EADS – evolution-associated difference spectrum; EET – excitation energy transfer; ESA – excited-state absorption; FCP – fucoxanthin–chlorophyll protein; IC – internal conversion; ICT – intramolecular charge-transfer; LHC – light-harvesting complex; PCP – peridinin–chlorophyll protein; SADS – species-associated difference spectrum; SE – stimulated emission

Introduction

Eukaryotic algae such as diatoms are vital for the ecology of oceanic systems, as they account for a large part of marine biomass production and photosynthetic activity. Like vascular plants, the eukaryotic diatoms possess only membrane-intrinsic photosynthetic pigment proteins. Their peripheral light-harvesting complex (LHC) has a high homology with the LHCII of green plants, but exhibits a distinct pigment composition (Büchel 2003). Like the plant antenna proteins, the ones from diatoms bind Chlorophyll *a* (Chl-*a*), but instead of the accessory Chl-*b* they contain Chl-*c*, and instead of lutein and neoxanthin in LHCII, the main carotenoids in the diatom antennae are fucoxanthin and diadinoxanthin. To improve the capturing of the green light which is available in the sea, the diatoms' LHC complex contains high stoichiometric amounts of fucoxanthin, and is thus called fucoxanthin–chlorophyll protein (FCP). FCP complexes are common among different

species of diatoms and brown algae, and it appears that the strategy of employing carotenoids rather than chlorophylls for the capturing of sunlight is usual among marine organisms, e.g. peridinin in the peridinin–chlorophyll protein (PCP) of dino-flagellates (Hofmann et al. 1996). Even though the crystal structure of FCP is not available, its homology with plant LHCII implies that it has a similar organization of the three transmembrane helixes. However, in contrast to the LHCII of higher plants, which binds 14 chlorophylls and 4 carotenoids (Liu et al. 2004), the FCP complex of diatoms binds chlorophylls and carotenoids with a 5:4 stoichiometry (see pigment analysis below), which together with sequence alignment observations (Eppard and Rhiel 1998) implies that the pigment binding sites may be only partly preserved.

Carotenoids serve multiple purposes in LHCs; their photo-protective and light-harvesting functions are of utter importance (Frank and Cogdell 1996). Carotenoids protect the organism against photodamage either by quenching the chlorophyll triplets before they can react with oxygen to form the highly reactive singlet oxygen, or by directly scavenging singlet oxygen and other dangerous radicals. Furthermore, carotenoids fill in the absorption spectrum of photosynthetic membranes by collecting the light in the blue/green region of the solar spectrum, where chlorophylls do not absorb. In general, the photon absorption by carotenoids is followed by the excitation energy transfer (EET) to chlorophylls (Polívka and Sundström 2004), from where the excitation energy finds its way to the reaction center (RC) protein where charge separation takes place (van Grondelle et al. 1994). The carbonyl group of fucoxanthin, which is conjugated with its backbone of 8 C=C, causes its excited-state dynamics to depend on the polarity of the environment, similar to other carbonyl-containing carotenoids (Zigmantas et al. 2004). In non-polar solvents, within $\sim$100 fs after excitation to the S_2 state, the excitation mostly resides on the 'normal' carotenoid S_1 state (the $2A^-_g$ state in C_{2h} symmetry), characterized by excited state absorption (ESA) around 530 nm and a decay of $\sim$70 ps, whereas in polar solvents, a low-lying intramolecular charge transfer (ICT) state is populated with significant yield, resulting in increased ESA above 600 nm and a shortening of the lifetime to $\sim$30 ps (Zigmantas et al. 2004).

In the LHCII of green plants, where Chl-a and Chl-b are the main light harvesting pigments, the transfer of energy from carotenoids to Chl-a, which is $\sim$80% efficient, proceeds mainly via their S_2 state ($>$60%) and to some extent from the S_1 state ($<$20%), and is thus observed on the time-scale of hundreds of femtoseconds to a few pico-seconds (Peterman et al. 1997; Gradinaru et al. 2000; Croce et al. 2001; van Amerongen and van Grondelle 2001). It has also been shown that the different carotenoids in LHCII may be coupled to either Chl-a or Chl-b, and thus utilize different EET pathways (Gradinaru et al. 2000; Croce et al. 2001). In LHCII, the EET dynamics is further complicated by the energy transfer from Chl-b to Chl-a which is also multi phasic, with components from 200 fs to 5 ps (van Amerongen and van Grondelle 2001; Novoderezhkin et al. 2004). For PCP, which is a structurally very different protein but like FCP contains high stoichiometric amounts of a carbonyl-containing carotenoid, it has been shown that peridinin is efficient in transferring energy to Chl-a (Bautista et al. 1999). However, in PCP, relatively little of the EET occurs via the S_2 state and the dominant pathways involve the lower excited states of peridinin (Krueger et al. 2001; Zigmantas et al. 2002). The energy transfer dynamics that take place in FCP have not been characterized, however, it has been shown that the combination of fucoxanthin with a multi-chlorophyll system results into efficient light harvesting (Büchel 2003).

To investigate the role and function of fucoxanthin in FCP and the pathways of EET in the complex after excitation, we performed ultrafast transient absorption experiments by selectively exciting fucoxanthin to its S_2 state.

Materials and methods

Protein preparation

FCPs were isolated as described earlier (Büchel 2003). In brief, isolated thylakoid membranes were solubilized at 0.125 mg Chl-a/ml with 10 mM β-1, 4-dodecyl maltoside (β-DDM, β-DDM/Chl-a = 41/1, w/w) for 20 min on ice and loaded on top of a continuous sucrose gradient achieved by a freeze–thaw cycle of a solution of 19% (w/v) sucrose in 10 mM Mes, pH 6.5, 2 mM KCl. Separation was

carried out by centrifugation using a swing-out rotor at 200,000 g for 16 h, which was shown to be sufficient to reach equilibrium. Two bands of brown color were obtained in the upper part of the gradient. The lower band was harvested, concentrated using Amicon filtrating devices with a cut-off of 30 kDa and stored at $-20°$ until use. The oligomeric state was checked on a gel filtration system according to the described procedure (Büchel 2003). The samples contained mostly higher oligomers accompanied by some trimers. This was confirmed by SDS-PAGE, demonstrating the presence of mainly the 19-kDa subunit and some 18-kDa subunits. Steady-state absorption, fluorescence and CD-spectra were scanned at room temperature as described in (Büchel 2003) demonstrating the functional intactness of the FCPs.

Pigment analysis

Pigment stoichiometries of isolated FCP sucrose density gradient bands (Table 1) were determined by analytical HPLC, after precipitation of the proteins and extraction of the pigments in 90% acetone (final concentration). Pigment species were separated on a reversed-phase column (Lichrosorb RP-18, 7 μm, 250 mm × 4 mm), using a two-step linear gradient from 80% methanol/20% H_2O to 60% methanol/40% acetone. Pigments were identified by their absorption spectra in solvent (on-line diode array detector, Waters). For quantification, calibration curves using the same HPLC system were obtained using pure Chl-c, fucoxanthin and diadinoxanthin purchased from DHI Water and Environment (Denmark). Chl-a was a kind gift from S. Hobe (Mainz). Pure pigments were first quantified spectroscopically, using their extinction coefficients and then injected onto the HPLC system and the respective peak areas were recorded. Chl-a was quantified in 80% acetone at 431 nm using an extinction coefficient of 95.82 l g^{-1} cm^{-1} (Lichtenthaler 1987). Chl-c was measured in 90% acetone at 444 nm ($\varepsilon = 374$ l/g/cm) (Jeffrey 1972). Fucoxanthin and diadinoxanthin concentrations were determined in 100% acetone at 448 nm ($\varepsilon = 166$ l g^{-1} cm^{-1} and 223 l g^{-1} cm^{-1}, respectively) (Johansen et al. 1974; Haugan et al. 1992).

Emission and fluorescence-excitation spectra

The steady-state emission and fluorescence excitation spectra of FCP were measured by using a commercial fluorometer (Jobin-Yvon Fluorolog 3) with right angle detection. The emission spectrum was collected with excitation at 460 nm and a detection bandwidth of 1 nm. For the fluorescence excitation spectrum, the excitation bandwidth was 1 nm and the fluorescence was detected at 680 nm.

Ultrafast transient absorption

Pump probe measurements were performed with an amplified Ti:sapphire laser system described in detail before (Gradinaru et al. 2000; Larsen et al. 2004). In brief, we used a Coherent-BMi a1000 system, which delivers a 1-kHz 795-nm pulse train; part of it drives the 60-fs visible non-collinear optical parametric amplifier (NOPA), which is used as a selective excitation light source (pump). Another part of the 795-nm light is used to generate single-filament white light supercontinuum in a translating CaF$_2$ disk, which serves as probe light over the entire visible range. An optical delay line allows for the precise timing of the pump and probe pulses, which are focused on the same spot ($\sim$120 μm diameter) in the continuously shaken, 1-mm pathlength, sample cuvette. Subsequently, the pump pulse is blocked and the probe is imaged on a diode-array detector. The intensity of the pump pulses was kept at $\sim$100 nJ per pulse and the relative polarization of the pump and probe beams was set at magic angle (54.7°). All measurements have been performed at 293 K.

Global and target analysis

The measured time and wavelength-resolved data have been analyzed globally (Holzwarth 1996; van Stokkum et al. 2004a, b). The analysis involves the correction of the data for the dispersion of the white light in the probe beam and the deconvolution of the instrument response function, which is

Table 1. Results of FCP pigment composition analysis[a]

Chl-a	Chl-c	Fucoxanthin	Diadinoxanthin
1	0.27 ± 0.06	0.97 ± 0.11	0.07 ± 0.03

[a] Numbers are given as mean values $\pm$ standard deviation of 15 independent measurements.

fitted with a gaussian. The application of a sequential model allowed us to estimate a set of evolution-associated difference spectra (EADS) and lifetimes capable of describing the temporal evolution of the data. Even though this model may capture the spectral evolution and the temporal behavior of the system, the EADS do not necessarily correspond to *pure*, but rather to mixtures of coexisting, excited states. To separate the contribution of the discrete excited states to the data, we need to apply a specific compartmental model in the target analysis (Holzwarth 1996; van Stokkum et al. 2004a, b). The prerequisite for such an analysis is the construction of a 'physical' model consisting of distinct compartments, which correspond to the states expected to participate in the observed dynamics; the dynamic processes are described by the population flow between these compartments, which can be sequential, parallel or bidirectional. By fitting the data to such a model we can estimate the species-associated difference spectra (SADS) and lifetimes, which correspond to the pure excited states.

Results and discussion

Characterization of the energy transfer in FCP by steady-state spectroscopy

The 1-Transmission (1-T) spectrum of FCP, shown in Figure 1 (dashed line), contains characteristic features of the three type of pigments that it contains; the Chl-*a* absorption appears at 670 nm (Q_y) and below 450 nm (Soret), the absorption of Chl-*c* appears at 635 nm (Q_y) and at 460 nm (Soret). The absorption of the fucoxanthins dominates in the 480–560 nm region and furthermore, (some of) the fucoxanthins are likely to absorb in the 420–470 nm region, where the absorption of FCP is rather high. The fucoxanthin and the Chl-*c* molecules play an important physiological role as their absorption covers the blue-green part of the solar spectrum, which dominates in marine environments. The fluorescence spectrum of FCP, which peaks at 674 nm, is independent of the excited pigment (Figure 1, solid line) and can be attributed solely to the emission of Chl-*a* (Büchel 2003). The fluorescence-excitation spectrum measured on FCP by detecting the Chl-*a* fluorescence above 680 nm (Figure 1, triangles), shows EET to
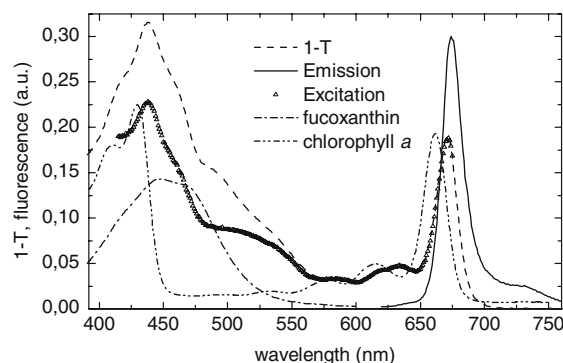
Figure 1. Room temperature 1-transmission (1-T), emission and fluorescence-excitation spectra of the FCP complex. The emission spectrum was measured with excitation at 460 nm and in the excitation spectrum the emission was detected above 680 nm. The emission spectra recorded with the excitation at 440, 510 and 625 nm were identical to the one shown. The 1-T spectra of Chl-*a* and fucoxanthin (dissolved in acetone and methanol, respectively) are also shown, to illustrate their contribution to the absorption of FCP.

Chl-*a* from the other pigments. The efficiency of EET from Chl-*c* is 100%; however, across the carotenoid absorption region the efficiency is non-uniform. This effect may be partly attributed to the presence of diadinoxanthin, but since this is present only in very small amounts (Table 1), it appears that there is at least one fucoxanthin which absorbs in the blue region and transfers energy poorly. If we compare FCP to the LHCII of plants, where carotenoids typically exhibit a 80% efficient EET (van Amerongen and van Grondelle 2001), the EET from fucoxanthin to Chl-*a* in FCP is less efficient, which is anticipated, as the amount of chlorophylls (i.e. potential acceptors) in FCP is significantly smaller than in LHCII. Figure 1 also contains the 1-T spectra of Chl-*a* and fucoxanthin measured in solution. To further understand the function of the different pigments and the mechanisms and pathways that are employed in the energy transfer, we have performed femtosecond transient absorption measurements.

Transient absorption dynamics in FCP

To study the EET properties of fucoxanthin in FCP, we have excited FCP with 530-nm laser pulses of ∼20 nm spectral width. As the absorption spectrum shows (Figure 1), at this wavelength we selectively excite the S_2 state of fucoxanthin. Figure 2 contains a set of kinetic traces that
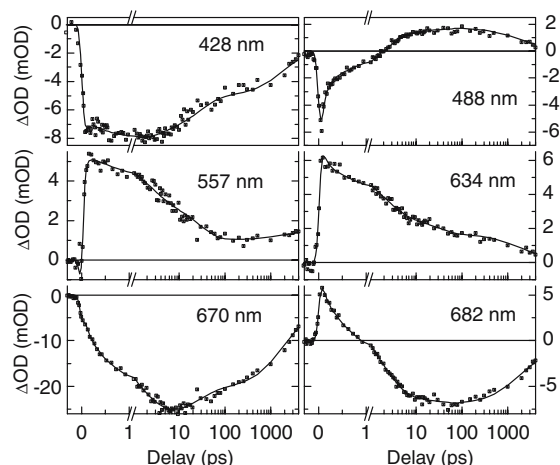
Figure 2. Transient absorption kinetic traces measured at various probe wavelengths after excitation of fucoxanthin in FCP with 530-nm pulses. The black squares denote the measured data points and the thin lines the fit to a sequential scheme of six compartments in global analysis.

illustrates the complexity of the processes that take place. At 428 nm, the signal is dominated by the bleach of the pigments; initially due to the excited fucoxanthins and at later times of the chlorophylls (Soret). At 488 nm, where at early times we mainly monitor the bleach of fucoxanthin, we observe a complex dynamics extending over different time-scales with the ESA of Chl-a dominating after 5 ps. At 557 nm, the signal at very early times is negative, corresponding to the SE of S_2. This is followed by the rise of a strong ESA, which most likely originates from the fucoxanthin S_1/ICT states. In this region chlorophyll also shows ESA, and thus the decay dynamics extends to longer timescales; furthermore, it is noteworthy, that at very late times (> 1 ns) the ESA signal at 557 nm increases. The trace measured at 634 nm, where Chl-c absorbs, follows the same trend of decay, without any obvious additional dynamics that could be attributed to the transient population of an excited state of Chl-c. The arrival of excitations on Chl-a is monitored by the strong negative signal around 670 nm, which consists of the bleach and the stimulated emission (SE). The signal shows a significant fast rise which is indicative of ultrafast EET, presumably from the fucoxanthin S_2 state. Further to the red, at 682 nm, at early times the data is dominated by the ESA of fucoxanthin which appears instantaneously, followed by the bleach/SE of Chl-a.

To estimate a set of EADS that can describe the transient absorption data measured after excitation of FCP at 530 nm, we have applied a sequential evolutionary scheme in global analysis; the results, EADS and lifetimes, are shown in Figure 3, while the fit kinetics are included in Figure 2 together with the measured traces. The region between 510 and 550 nm is contaminated by the scattering of excitation light and has been omitted from the analysis. Six components were needed for achieving a good fit, with lifetimes ranging from sub-100 fs to non-decaying (Figure 3).

In the blue region of the spectrum, the spectral evolution shows that at early times fucoxanthin is found in the S_2 state. The bleach and SE features dominate the displayed region (up to 510 nm). In several successive steps (75 fs, 620 fs, 2.5 ps), the bleach in the 450–510 nm region disappears indicating that the fucoxanthins have decayed to the ground state. The late EADS in that region have Chl-a characteristics; bleach below 450 nm and flat ESA around 450–500 nm.

Further to the red, the EADS are dominated by ESA features and the superimposed bleach of the Chl-a Q_y band at 670 nm. In the 1st EADS (thin solid line), the ESA is progressively increasing towards the red, depicting the S_2 ESA which for carotenoids typically appears in the near infrared (Zhang et al. 2001; Papagiannakis et al. 2003). The ESA is decreasing in the successive EADS denoting the loss of excited fucoxanthins in the sub-picosecond and picosecond timescale and of Chl-a at later times. It is noteworthy, that the Chl-a 670-nm bleach is present with significant amplitude already in the 1st EADS. This suggests that the
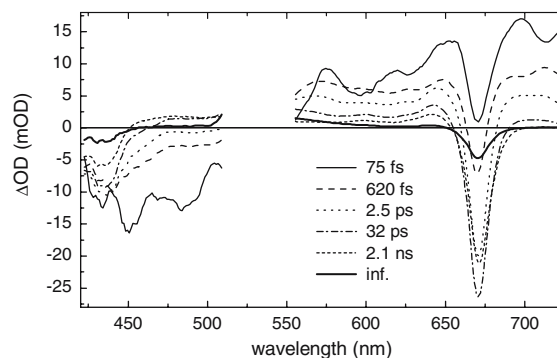
Figure 3. The EADS and lifetimes estimated by a sequential scheme in global analysis of the transient absorption data measured after excitation of fucoxanthin in FCP by 530-nm pulses.

EET from the S_2 state of at least one of the fucoxanthins to Chl-a is extremely rapid and that the contributions of the two species (fucoxanthin S_2 and excited Chl-a) to the data cannot be resolved (see also the 670-nm kinetic trace in Figure 2). The 1st EADS also shows a peculiar shape around 600–630 nm, where Chl-c shows its absorption; even though it is tempting to assign this shape to an involvement of Chl-c in the ultrafast fucoxanthin–Chl-a EET, we have to point out that the details of this EADS, which appears upon excitation, are prone to uncertainty due to inaccuracies in the determination of the dispersion in the white light probe beam and also experimental artifacts around time zero. Furthermore, we do not observe a distinct bleach feature at 460 nm, which would signify the excitation of Chl-c.

The 2nd and 3rd EADS (dashed and dotted lines) contain the broad ESA of the lower excited states of fucoxanthin together with the Chl-a Q_y bleach at 670 nm. The 620 fs decay of the 2nd EADS corresponds to a significant increase of Q_y bleach indicative of efficient EET from this intermediate. The Q_y bleach is further increased in the following step of 2.5 ps, which in the ESA region has a shape similar to that of its predecessor, albeit reduced amplitude. A sub-picosecond EET step was also observed in PCP where it was ascribed to EET from vibrationally hot or unrelaxed S_1/ICT states (Zigmantas et al. 2002). In this time range the fucoxanthin ESA is very broad, reminiscent of the ESA of fucoxanthin in a polar solvent (Zigmantas et al. 2004) and of peridinin in PCP (Krueger et al. 1999). No distinct ESA bands are observed, and therefore it is not possible to draw any conclusions about the relation (Papagiannakis et al. 2004) and, possibly discrete, role of the S_1 and ICT states in FCP, other than that they are likely to co-exist.

The 4th and 5th EADS (dash-dot, short dash lines) are largely characterized by Chl-a features: strong 670-nm bleach and flat ESA elsewhere. However, the 32-ps decay of the 4th EADS corresponds to spectral changes that are indicative of the coexistence of more species, namely a fucoxanthin S_1 state: in the region where the Chl-a ESA overlaps with the bleach of fucoxanthin (450–510 nm), the 4th EADS has relatively smaller amplitude than the 5th EADS. This implies that a fraction of the fucoxanthin population does not participate in the fast EET processes but either

transfers energy to Chl-a much slower or decays to the ground state with its intrinsic lifetime of $\sim$30 ps (Zigmantas et al. 2004). The 5th EADS is the 'pure' spectrum of Chl-a in FCP. Given the presence of four Chl-a molecules in FCP, the Chl-a population is likely to exhibit, apart from its natural decay dynamics, some additional decay components (Gobets et al. 2001) which will be further complicated by singlet–singlet annihilation (van Grondelle 1985), even though the excitation power levels were kept low.

The final, 6th, EADS (thick solid line) does not decay in the time window of our measurement and describes an increase of ESA below 560 nm. Even though due to the pump scatter it is not possible to obtain the complete spectral shape associated with this dynamics, the observed spectral features point to the formation of the triplet state of fucoxanthin, which is expected to appear in this spectral region (Osuka et al. 1999) on the nanosecond timescale after the quenching of chlorophyll triplets formed by intersystem crossing. Notably, this EADS also contains a negative feature in the Chl-a Q_y region; this effect, which has also been observed in plant LHCII complexes (Peterman et al. 1995), indicates that either the chlorophyll triplets are not fully quenched in this time window, or that there is an interaction between the fucoxanthin triplet and the chlorophylls, causing the chlorophyll to display a spectral response, while the fucoxanthin is in its triplet state.

The above analysis indicates that fucoxanthin in FCP exhibits a behavior similar to that of peridinin in PCP in achieving efficient EET. As is apparent from the 1st EADS, which contains a Chl-a bleach of considerable magnitude, a significant fraction of the total EET is mediated on an extremely short timescale. It could be argued that at 530 nm we directly excite a higher (electronic or vibronic) level of one of the chlorophylls, however, at this wavelength this should only be a weak absorption (Figure 1) which cannot contribute such a large feature to the transient absorption spectrum. Following the decay of S_2, part of the excitation decays to the lower singlet excited states of fucoxanthin, presumably a mixture of the S_1 and ICT states (Zigmantas et al. 2004). The analysis allows us to conclude that efficient EET occurs also from these lower states as their lifetime is significantly shortened relative to that measured in an organic solvent, which is between 30 and 60 ps

(Zigmantas et al. 2004). The EET from fucoxanthin to Chl-a in FCP also involves a sub-picosecond intermediate step, reminiscent of that observed in other LHCs where it was assigned to EET from 'hot' or unrelaxed intermediates (Papagiannakis et al. 2002; Walla et al. 2002; Zigmantas et al. 2002). Even though this sub-picosecond compartment seems to be contributing considerably to the EET, it is not possible to directly determine what fraction of EET is mediated in this fast phase and what in the 2.5-ps phase, as the observed dynamics is a mixture of the increase of Chl-a signals (bleach and ESA) and the loss of the ESA of fucoxanthin.

We also point out the absence of a spectral evolution in the Chl-a region; the Q_y bleach appears at 670 nm and does not exhibit any spectral shift. As a consequence, not much can be said about the energy transfer dynamics among the Chl-a's in FCP. However, the lack of spectral dynamics does suggest that the four Chl-a molecules are spectroscopically rather equivalent and weakly interacting.

To separate the aforementioned different processes we need to resort to target analysis which allows us to model parallel and uncoupled processes among discrete excited species, each one of which is characterized by a SADS.

Compartmental modeling: relating dynamics and structure

The analysis of the data with a sequential model like above, provides a qualitative description of the processes that follow the excitation of fucoxanthin in FCP with 530 nm pulses. However, the spectrally overlapping bands and the continuous spectral evolution hinder the full interpretation of the underlying events. To separate the processes that take place and identify the excited states involved, we have performed a target analysis (van Stokkum et al. 2004a). To fit the data well and accommodate all the spectral and temporal aspects of the system, it was essential to use a model of 8 compartments, which is shown in Figure 4 and illustrates the complexity of the processes that take place in the FCP antenna. We have used four compartments to describe the singlet excited states of fucoxanthin. They correspond to the initially excited S_2 state and the lower states which we presume are a mixture of the S_1 and ICT states. On
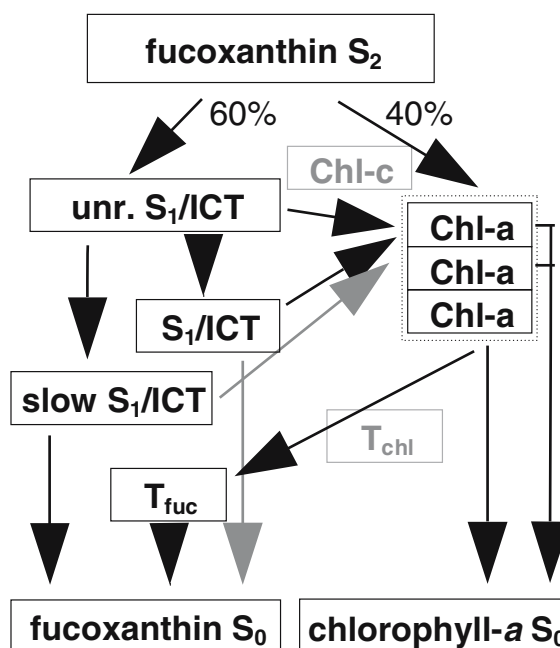
Figure 4. The compartmental scheme that we used to model the energy transfer network in FCP. The grey arrows depict the least efficient pathways of energy flow. The Chl-a compartments describe the continuous decay observed in the signal and not necessarily different molecules. We have not observed a contribution of Chl-c or of the Chl-a triplet state; for the sake of completeness we include the corresponding compartments in light grey.

the basis of our data, we cannot address the S_1/ICT connectivity and, we thus describe them as one compartment, although this is most likely an oversimplification (Papagiannakis et al. 2004). From the ESA evolution we can resolve three additional phases: the first denotes a 'hot' or 'unrelaxed' intermediate, the second the S_1/ICT states that transfer energy efficiently, while the third fraction corresponds to an S_1/ICT population that is not transferring energy, or is doing so rather slowly. The Chl-a excited state evolution is described by three discrete compartments which are interconnected sequentially; furthermore, each of the three compartments is allowed to decay to the ground state. This has been essential for capturing the continuous loss of Chl-a signal; this may partly originate from the different chlorophylls in the complex exhibiting vastly different lifetimes as a result of different configuration and/or environment, and moreover, as mentioned earlier, multiple decays are needed to describe the annihilation processes that may be taking place. The final state of the system is described by the fucoxanthin

triplet state, which appears after the quenching of the Chl-*a* triplet. The latter is not observed directly, and therefore it is marked with light gray in the model. The Chl-*c* is also represented by a compartment, but as we have no evidence that it participates in the fucoxanthin–Chl-*a* EET, it is not connected to any process and appears also in light gray.

To estimate reliable and physical SADS in such a compartmental scheme, it is necessary to limit the solution space by fixing some of the rate constants and applying some spectral constraints. Here, we have applied the following restrictions: (A) the S_2 lifetime has been fixed to 75 fs, as it cannot be determined accurately by our 100-fs time resolution; (B) The branching from S_2 (IC/EET) has been adjusted so that the resulting fucoxanthin SADS were devoid of Chl-*a* contributions in the 670-nm region; we found a branching IC/EET ratio of 60:40 to be the best solution; (C) the SADS of the S_1/ICT and the non/slow-transferring S_1/ICT states have been restricted to have the same shape; and (D) the SADS of the fucoxanthin triplet state has been imposed to be zero above 635 nm, so as to avoid compensation effects with the Chl-*a* bleach.

The target analysis SADS are shown in Figure 5: the upper panel contains the fucoxanthin SADS and the lower the Chl-*a* SADS. Furthermore, the dynamics of the singlet excited states of fucoxanthin and Chl-*a* are summarized in Table 2. We have been successful in separating the different species, as the SADS are characteristic of the excited states. Only the SADS of the S_2 state contains a Chl-*a* bleach, which as discussed earlier, indicates that, at least a part of the S_2–Chl-*a* EET is so fast that it cannot be separated from the SADS of the S_2 state itself, like in PCP (Krueger et al. 2001). We suggest that this ultrafast phase corresponds to one fucoxanthin favorably positioned with respect to one or more Chl-*a*s. The SADS of the S_1/ICT states show a broad ESA that covers the visible range. There seem to be two bands in the ESA, at 570 and 680 nm, which could correspond to the contributions of the S_1 and ICT states, like those observed on fucoxanthin in solution (Zigmantas et al. 2004). The Chl-*a* SADS, which contain the bleach of the Soret and Q_y absorption bands and a broad ESA, do not exhibit any spectral evolution (Figure 5, lower panel), demonstrating that the Chl-*a* molecules are weakly interacting. Furthermore, these SADS do not
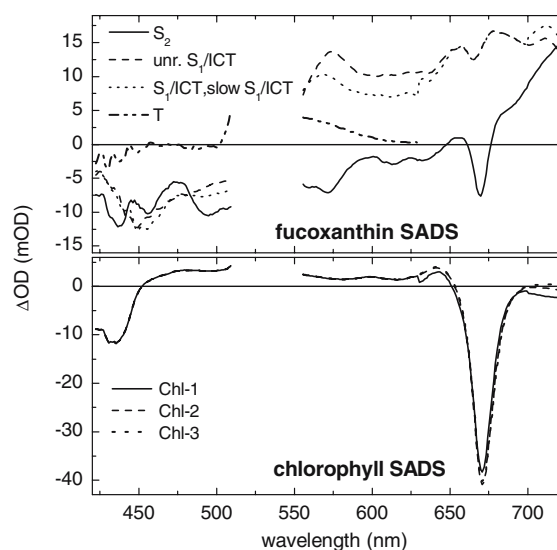
Figure 5. Target analysis SADS corresponding to the discrete states described in the compartmental scheme of Figure 4. The upper panel contains the SADS of the excited states of fucoxanthin and the lower panel the SADS of Chl-*a*.

contain any signature of a fucoxanthin response, similar to the response of that carotenoids exhibit in LH2 (Herek et al. 1998) or PCP (Salverda 2003) when the (bacterio)chlorophylls in the complex are excited, which implies that the electrostatic interactions between the Q_y of Chl-*a* and the fucoxanthins are weak. In the model, the EET efficiency of the fucoxanthin sub-population which is excited at 530 nm approaches 80%, in consistence with the fluorescence excitation spectrum in that spectral region (Figure 1).

In these room temperature measurements, we find no clear indication for an involvement of Chl-*c* in the fucoxanthin–Chl-*a* EET. Low-temperature measurements which will offer increased spectral resolution are needed for answering this question. When Chl-*c* was excited directly at 630 nm (data not shown) we observed that the EET to Chl-*a* was extremely fast and could not be resolved as it was complete within ~100 fs.

If we use these findings to relate the structure of the FCP complex to the LHCII complex of higher plants (Liu et al. 2004), with which it shares a homology (Eppard and Rhiel 1998), we can first conclude that the pigment composition is most likely to be 4:4:1 (Chl-*a*, fucoxanthin, Chl-*c*) rather than 8:8:2. If the latter was true, the Chl-*a* Q_y absorption should be red-shifted due to excitonic interactions (van Amerongen and van Grondelle

Table 2. Results of target analysis[a]

	S$_2$	Unrelaxed S$_1$/ICT	S$_1$/ICT	Slow S$_1$/ICT	Chl-*a*
Lifetime[b]	75 fs	320 fs	2.6 ps	31 ps	7.5 ps, 112 ps, 3.9 ns
Efficiency %	40%	20%	90%	5%	

[a] The lifetimes and the energy transfer efficiencies estimated by target analysis. The first four columns correspond to the excited states of fucoxanthin and the fifth to the Chl-*a* compartments. The % efficiency refers to the fraction of the population of the specific state that goes to Chl-*a*.
[b] The error in estimating the lifetimes within the specific model is ±5%.

2001; Novoderezhkin et al. 2004) and not at 670 nm; furthermore, it seems highly unlikely that the protein would be accommodating 8 fucoxanthin molecules. The FCP and LHCII sequence alignment (Eppard and Rhiel 1998) shows that five of the chlorophyll binding sites in LHCII are preserved in FCP; a1, a2, a3, a4, a5 (corresponding to a610, a612, a613, a602 and a603 in Liu et al. 2004). It thus seems that the FCP has kept the essential core of four chlorophylls (a1, a2, a4, a5). In the LHCII structure, there is at least one carotenoid molecule that is very well coupled to those chlorophylls; in a similar way in FCP, this might correspond to a fucoxanthin that achieves extremely fast EET from its S$_2$ state. The fluorescence excitation spectrum measured on FCP suggests that there is at least one fucoxanthin, which is rather blue-shifted and is rather poor in EET. Even though on the basis of the sequence it is only known that two central lutein-binding sites of LHCII are most probably preserved in FCP (Green and Kühlbrandt 1995), we might speculate about the binding sites of the two other fucoxanthins. In higher plant LHCII, both additional xanthophylls are situated in niches made of amino acid side chains and of chlorophylls. In FCP, the respective amino acids as well as the chlorophylls are not conserved, except for chlorophyll a3/613 in case of the binding niche of the fourth xanthophyll. Thus, the binding of the two additional fucoxanthin molecules may differ from the situation in higher plants. As less chlorophylls are bound to FCP, it is highly likely that one of the fucoxanthins is bound in an area where chlorophylls are absent; this would result in this fucoxanthin being disconnected from the energy transfer network in FCP. The observation that the Chl-*c*–Chl-*a* EET is extremely fast indicates that the Chl-*c* molecule is bound in one of the four core sites rather than at site a3/a613; this site in FCP binds a Chl-*a*, as in LHCII.

Concluding remarks

We have studied the FCP complex of the diatom *Cyclotella meneghiniana*. The pigment analysis indicates that this protein binds significantly less chlorophylls than the LHCII complex of green plants, and thus relies much stronger on the harvesting of light by its carotenoid, fucoxanthin. Our Fluorescence-excitation measurement indicates that the energy transfer from Chl-*c* to Chl-*a* is 100% efficient, but also that not all four fucoxanthins in the complex are equally efficient. A transient absorption measurement with excitation of the S$_2$ state of fucoxanthin at 530 nm and subsequent modeling by target analysis, has allowed us to characterize the energy transfer network in FCP and then relate it to its pigment organization. After the excitation of fucoxanthin at 530 nm, we observe efficient EET to Chl-*a*, which occurs in multiple steps. We also observe a fraction that is not, or is poorly, transferring energy to Chl-*a*. The lack of spectral evolution in the Chl-*a* bleach band and the fact that it appears at 670 nm, indicate that the chlorophylls in the FCP complex are not excitonically coupled like in LHCII. The observation that the Chl-*c*–Chl-*a* EET is extremely fast and hints that the Chl-*c* molecule is bound in a site adjacent to that of Chl-*a* molecules.

References

Büchel C (2003) Fucoxanthin–chlorophyll proteins in diatoms: 18 and 19 kDa subunits assemble into different oligomeric states. Biochemistry 42: 13027–13034

Croce R, Muller MG, Bassi R and Holzwarth AR (2001) Carotenoid-to-chlorophyll energy transfer in recombinant major light-harvesting complex (LHCII) of higher plants. I. Femtosecond transient absorption measurements. Biophys J 80: 901–915

Eppard M and Rhiel E (1998) The genes encoding light-harvesting subunits of *Cyclotella cryptica* (Bacillariophyceae)

constitute a complex and heterogeneous family. Mol Gen Genet 260: 335–345

Frank HA and Cogdell RJ (1996) Carotenoids in photosynthesis. Photochem Photobiol 63: 257–264

Gobets B, Kennis JTM, Ihalainen JA, Brazzoli M, Croce R, van Stokkum IHM, Bassi R, Dekker JP, van Amerongen H, Fleming GR and van Grondelle R (2001) Light harvesting by chlorophylls and carotenoids in the Photosystem I core complex of *Synechococcus elongatus*: a fluorescence upconversion study. J Phys Chem B 104: 4485–4494

Gradinaru CC, van Stokkum IHM, Pascal AA, van Grondelle R and van Amerongen H (2000) Identifying the pathways of energy transfer between carotenoids and chlorophylls in LHCII and CP29. A multicolor, femtosecond pump-probe study. J Phys Chem B 104: 9330–9342

Green BR and Kühlbrandt W (1995) Sequence conservation of light-harvesting and stress-response proteins in relation to the three-dimensional molecular structure of LHCII. Photosynth Res 44: 139–148

Haugan JA, Englert G, Glinz E and Liaaenjensen S (1992) Algal carotenoids. 48. Structural assignments of geometrical-isomers of fucoxanthin. Acta Chem Scand 46: 389–395

Herek JL, Polivka T, Pullerits T, Fowler GJS, Hunter CN and Sundström V (1998) Ultrafast carotenoid band shifts probe structure and dynamics in photosynthetic antenna complexes. Biochemistry 37: 7057–7061

Hofmann E, Wrench PM, Sharples FP, Hiller RG, Welte W and Diederichs K (1996) Structural basis of light harvesting by carotenoids: peridinin-chlorophyll-protein from *Amphidinium carterae*. Science 272: 1788–1791

Holzwarth AR (1996) Data analysis of time-resolved measurements. In: Amesz J and Hoff AJ (eds) Biophysical Techniques in Photosynthesis, pp 75–92. Kluwer Academic Publishers, Dordrecht, The Netherlands

Jeffrey SW (1972) Preparation and some properties of crystalline chlorophyll-C1 and C2 from marine algae. Biochim Biophys Acta 279: 15–33

Johansen JE, Svec WA, Liaaenje S and Haxo FT (1974) Algal carotenoids. 10. Carotenoids of Dinophyceae. Phytochemistry 13: 2261–2271

Krueger BP, Yom J, Walla PJ and Fleming GR (1999) Observation of the S_1 state of spheroidene in LH2 by two-photon fluorescence excitation. Chem Phys Lett 310: 57–64

Krueger BP, Lampoura SS, van Stokkum IHM, Papagiannakis E, Salverda JM, Gradinaru CC, Rutkauskas D, Hiller RG and van Grondelle R (2001) Energy transfer in the peridinin chlorophyll-a protein of *Amphidinium carterae* studied by polarized transient absorption and target analysis. Biophys J 80: 2843–2855

Larsen DS, Vengris M, van Stokkum IHM, van der Horst M, de Weerd FL, Hellingwerf KJ and van Grondelle R (2004) Photoisomerization and photoionization of the photoactive yellow protein chromophore in solution. Biophys J 86: 2538–2550

Lichtenthaler HK (1987) Chlorophylls and carotenoids – pigments of photosynthetic biomembranes. Meth Enzymol 148: 350–382

Liu ZF, Yan HC, Wang KB, Kuang TY, Zhang JP, Gui LL, An XM and Chang WR (2004) Crystal structure of spinach major light-harvesting complex at 2.72 Å resolution. Nature 428: 287–292

Novoderezhkin VI, Palacios MA, van Amerongen H and van Grondelle R (2004) Energy-transfer dynamics in the LHCII complex of higher plants: modified redfield approach. J Phys Chem B 108: 10363–10375

Osuka A, Kume T, Haggquist GW, Javorfi T, Lima JC, Melo E and Naqvi KR (1999) Photophysical characteristics of two model antenna systems: a fucoxanthin-pyropheoporbide dyad and its peridinin analogue. Chem Phys Lett 313: 499–504

Papagiannakis E, Kennis JTM, van Stokkum IHM, Cogdell RJ and van Grondelle R (2002) An alternative carotenoid-to-bacteriochlorophyll energy transfer pathway in photosynthetic light harvesting. Proc Natl Acad Sci USA 99: 6017–6022

Papagiannakis E, van Stokkum IHM, van Grondelle R, Niederman RA, Zigmantas D, Sundström V and Polívka T (2003) A near-infrared transient absorption study of the excited-state dynamics of the carotenoid spirilloxanthin in solution and in the LH1 complex of *Rhodospirillum rubrum*. J Phys Chem B 107: 11216–11223

Papagiannakis E, Larsen DS, van Stokkum IHM, Vengris M, Hiller R and van Grondelle R (2004) Resolving the excited state equilibrium of peridinin in solution. Biochemistry 43: 15303–15309

Peterman EJG, Dukker FM, van Grondelle R and van Amerongen H (1995) Chlorophyll a and carotenoid triplet states in light-harvesting complex II of higher plants. Biophys J 69: 2670–2678

Peterman EJG, Monshouwer R, van Stokkum IHM, van Grondelle R and van Amerongen H (1997) Ultrafast singlet excitation transfer from carotenoids to chlorophylls via different pathways in light-harvesting complex II of higher plants. Chem Phys Lett 264: 279–284

Polívka T and Sundström V (2004) Ultrafast dynamics of carotenoid excited states. From solution to natural and artificial systems. Chem Rev 104: 2021–2071

Salverda JM (2003) Interacting pigments in light-harvesting complexes studied with nonlinear spectroscopy. PhD thesis, Vrije Universiteit, Amsterdam

van Amerongen H and van Grondelle R (2001) Understanding the energy transfer function of LHCII, the major light-harvesting complex of green plants. J Phys Chem B 105: 604–617

van Grondelle R (1985) Excitation energy transfer, trapping and annihilation in photosynthetic systems. Biochim Biophys Acta 811: 147–195

van Grondelle R, Dekker JP, Gillbro T and Sundström V (1994) Energy-transfer and trapping in photosynthesis. Biochim Biophys Acta 1187: 1–65

van Stokkum IHM, Larsen DS and van Grondelle R (2004a) Global and target analysis of time-resolved spectra. Biochim Biophys Acta 1657: 82–104

van Stokkum IHM, Larsen DS and van Grondelle R (2004b) Erratum to "Global and target analysis of time-resolved spectra". Biochim Biophys Acta 1658: 82–104

Walla PJ, Linden PA, Ohta K and Fleming GR (2002) Excited-state kinetics of the carotenoid S_1 state in LHC II and two-photon excitation spectra of lutein and beta-carotene in solution: efficient car $S_1 \rightarrow$ Chl electronic energy transfer via hot S_1 states? J Phys Chem A 106: 1909–1916

Zhang JP, Skibsted LH, Fujii R and Koyama Y (2001) Transient absorption from the $1B_u^-$ state of all-trans-beta-carotene newly identified in the near-infrared region. Photochem Photobiol 73: 219–222

Zigmantas D, Hiller RG, Sharples FP, Frank HA, Sundstrom V and Polívka T (2004) Effect of a conjugated carbonyl group on the photophysical properties of carotenoids. Phys Chem Chem Phys 6: 3009–3016

Zigmantas D, Hiller RG, Sundström V and Polívka T (2002) Carotenoid to chlorophyll energy transfer in the peridinin-chlorophyll-a-protein complex involves an intramolecular charge transfer state. Proc Natl Acad Sci USA 99: 16760–16765